

Chapter 16

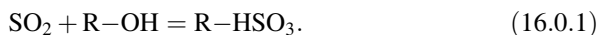
Absorption–Adsorption Method



Different companies (Babcock & Wilcox Power Generation Group, Inc., Alstom Power Italy, Idreco-Insigma-Consortium) propose methods and apparatuses for waste gas purification from SO_2 using two-phase absorbent (CaCO_3 suspension). The adsorption (absorption) of SO_2 on materials derived from natural carbonates [1–3] has the drawback of waste accumulation. The basic problem of the carbonate absorbents is that its chemical reaction with SO_2 lead to CO_2 emission (every molecule of SO_2 absorbed from the air is equivalent to a molecule of CO_2 emitted in the air), because the ecological problems (greenhouse effects) of SO_2 and CO_2 are similar. The large quantity of by-products is a problem, too. Another drawback of these methods is the impossibility for regeneration of the absorbents.

The theoretical analysis [4–10] of the method and apparatus for waste gas purification from SO_2 using two-phase absorbent (CaCO_3 suspension) shows that the process in the absorption column in the gas–liquid drops flow is practically physical absorption as a result of the low concentration of the dissolved CaCO_3 and SO_2 in the drops and its brief existence in the gas–liquid dispersion. An increase of the process efficiency is proposed in the patent [11], where an absorption column with two absorption zones (lower liquid–gas bubbles zone and upper gas–liquid drops zone) is used. The effect is the possibility to increase the absorption degree or to lower the column height.

The use of synthetic anionites (basic anion-exchange resins— R-OH form of Amberlite, Duolite, Kastel, Varion, Wofatit) as adsorbents [12–14] for gas purification from SO_2 provides possibilities for adsorbent regeneration. The chemical reaction of SO_2 with the synthetic anionites in gas–solid systems can be presented by the stoichiometric equation

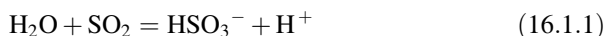


After saturation of the synthetic anionite particles with sulfur dioxide, the adsorbent regeneration is possible to be carried out with water solution of NH_4OH :

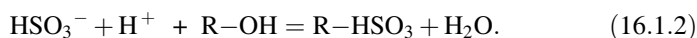


16.1 Two-Step Absorption–Adsorption Method

The main disadvantages of the CaCO_3 suspension method (CO_2 emission, gypsum accumulation and inability to regenerate the adsorbent) are handled by the patent [15] (see Fig. 16.1), where the waste gas purification is realized in two steps, i.e., physical absorption of SO_2 with water



and chemical adsorption of HSO_3^- from the water solution by synthetic anionite particles:



The adsorbent regeneration is made with NH_4OH solution [see (16.0.2)]. The obtained $(\text{NH}_4)_2\text{SO}_3$ (NH_4HSO_3) is used (after reaction with HNO_3) for production of concentrated SO_2 (gas) and NH_4NO_3 (solution).

In Fig. 16.1, the gas enters in the middle part of the column 2 through the inlet 1, gets in contact with the absorbent (H_2O) in the upper part of the column, where a gas–liquid drops countercurrent flow is formed, passes through the liquid drops separator 4, and out through the outlet 5. The absorbent enters the column through the inlets 11 and spreader 3, absorbs the SO_2 from the gas in the middle part of the column, collects at the bottom of the column, and goes out through the exit 6. After that, the absorbent ($\text{H}_2\text{O} + \text{SO}_2$) passes through one of the valves 7 and enters in one of the adsorbers 8, where SO_2 is adsorbed on the particles of synthetic anionite and the regenerated absorbent (H_2O) is returned by pumps 9 and valves 10 to the absorption column through the inlets 11.

The absorbent, separated in the separator 4, passes through the outlets 12 and valve 13 and enters the adsorbers 8.

After the synthetic anionite particles have been saturated with sulfur dioxide in the adsorbers 8, the adsorbent regeneration is realized by means of water solution of NH_4OH , which is obtained in the NH_3 absorber 14 and through the pump 15 and the valves 16 enters the adsorbers 8. The water solution of $(\text{NH}_4)_2\text{SO}_3$ obtained in 8 (after adsorbent regeneration) enters through the pumps 9 and valves 17 in the reactor 18, where it reacts with HNO_3 (coming from the tank 19). The obtained concentrated SO_2 (gas) and NH_4NO_3 solution goes out of the system through the outlet 21. The pump 20 allows the solution of $(\text{NH}_4)_2\text{SO}_3$ to be re-circulated in order to achieve higher concentration. The absorber 2 is possible to be replaced by a bi-zonal absorber (see Fig. 15.1).

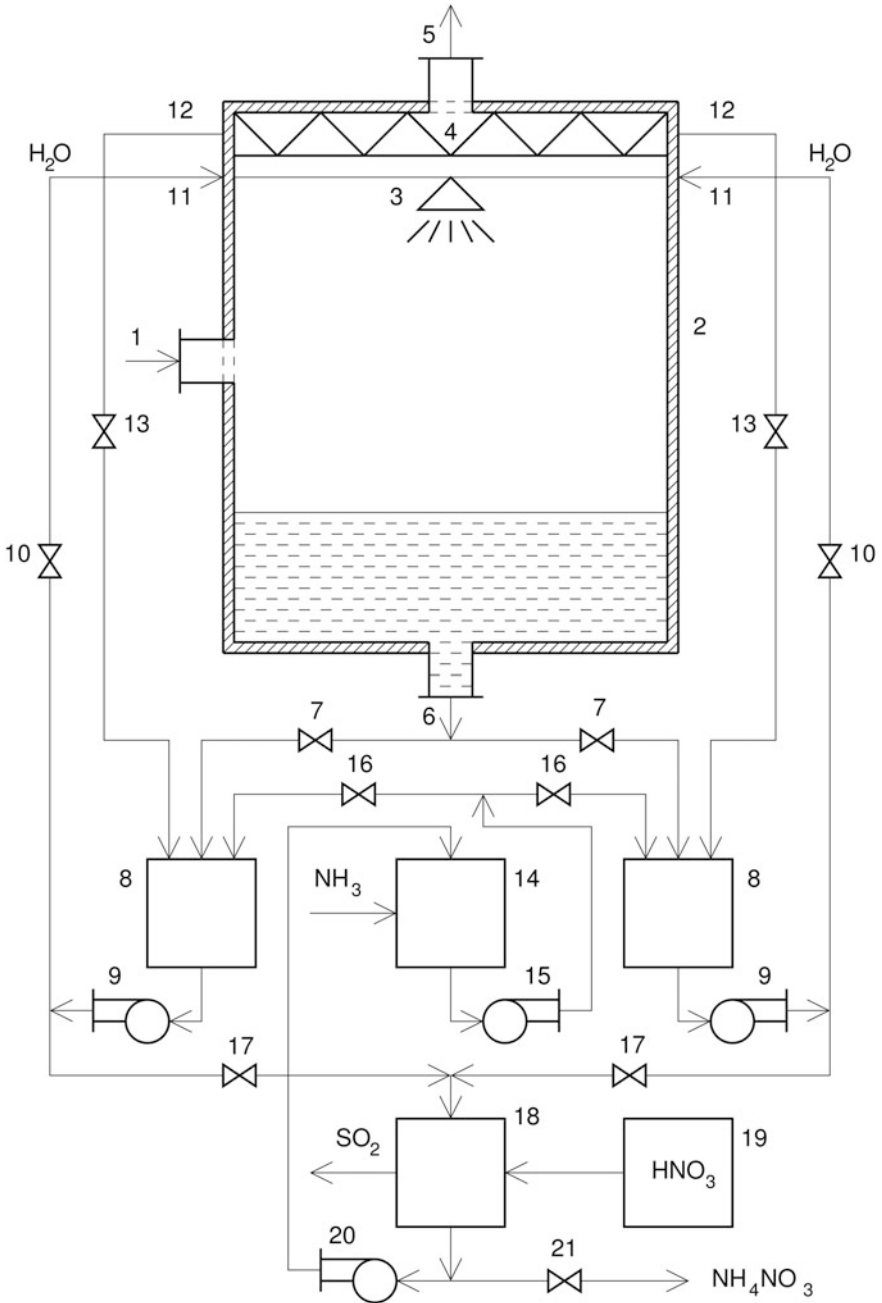


Fig. 16.1 Absorption-adsorption approach

The main processes in the absorption-adsorption method are the physical absorption of SO₂ by H₂O in a countercurrent gas-liquid drops system and a chemical adsorption of SO₂ by synthetic anionite particles in a liquid-solid system.

16.2 Absorption and Adsorption Modeling

The modeling of a non-stationary (as a result of the adsorbent saturation) absorption-adsorption cycle of the method for gas purification from SO₂ uses a combination of the physical absorption model (3.1.2) and (3.1.3) and chemical adsorption model (3.2.18) and (3.2.19):

$$\begin{aligned}
 \frac{\partial c_1}{\partial t} + u_1 \frac{\partial c_1}{\partial z_1} &= D_1 \left(\frac{\partial^2 c_1}{\partial z_1^2} + \frac{1}{r_1} \frac{\partial c_1}{\partial r_1} + \frac{\partial^2 c_1}{\partial r_1^2} \right) - k_0(c_1 - \chi c_2); \\
 \frac{\partial c_2}{\partial t} + u_2 \frac{\partial c_2}{\partial z_2} &= D_2 \left(\frac{\partial^2 c_2}{\partial z_2^2} + \frac{1}{r_1} \frac{\partial c_2}{\partial r_1} + \frac{\partial^2 c_2}{\partial r_1^2} \right) + k_0(c_1 - \chi c_2); \\
 t = 0, \quad c_1 &\equiv c_1^0, \quad c_2 \equiv 0; \\
 r_1 = 0, \quad \frac{\partial c_1}{\partial r_1} &= \frac{\partial c_2}{\partial r_1} \equiv 0; \quad r_1 = r_{10}, \quad \frac{\partial c_1}{\partial r_1} = \frac{\partial c_2}{\partial r_1} \equiv 0; \\
 z_1 = 0, \quad c_1(r_1, 0) &\equiv c_1^0, \quad u_1^0 c_1^0 \equiv u_1(r_1) c_1^0 - D_1 \left(\frac{\partial c_1}{\partial z_1} \right)_{z_1=0}; \\
 z_2 = 0, \quad c_2(r_1, 0) &\equiv \bar{c}_{12}(l_2), \quad u_2^0 \bar{c}_{12}(l_2) \equiv u_2(r_1) \bar{c}_{12}(l_2) - D_2 \left(\frac{\partial c_2}{\partial z_2} \right)_{z_2=0}.
 \end{aligned} \tag{16.2.1}$$

$$\begin{aligned}
 \frac{\partial c_{12}}{\partial t} + u \frac{\partial c_{12}}{\partial z} &= D_{12} \left(\frac{\partial^2 c_{12}}{\partial z^2} + \frac{1}{r} \frac{\partial c_{12}}{\partial r_2} + \frac{\partial^2 c_{12}}{\partial r_2^2} \right) - k_1(c_{12} - c_{13}); \\
 \frac{dc_{13}}{dt} &= k_1(c_{12} - c_{13}) - k c_{13} c_{23}; \quad \frac{dc_{23}}{dt} = -k c_{13} c_{23}; \\
 t = 0, \quad c_{12} &\equiv 0, \quad c_{13} \equiv 0, \quad c_{23} \equiv c_{23}^0; \\
 r_2 = 0, \quad \frac{\partial c_{12}}{\partial r_2} &\equiv 0; \quad r_2 = r_{20}, \quad \frac{\partial c_{12}}{\partial r_2} \equiv 0; \\
 z = 0, \quad c_{12}(r_2, 0) &\equiv \bar{c}_2(l_1), \quad u^0 \bar{c}_2(l_1) \equiv u(r_2) \bar{c}_2(l_1) - D_2 \left(\frac{\partial c_{12}}{\partial z} \right)_{z=0}.
 \end{aligned} \tag{16.2.2}$$

In the absorber model (16.2.1), c_1 , c_2 , D_1 , D_2 are the concentrations and diffusivities of SO₂ in the gas and liquid phases, u_1 , u_2 —the velocities in the gas and liquid phases, r_1 , l_1 —the radius and height of the working zone of the column, t —the time. In the adsorber model (16.2.2), c_{12} , D_{12} are the concentration and diffusivity of SO₂ in the liquid phase in the adsorber, c_{13} , c_{23} —the concentrations of

SO₂ and active sites in the adsorbent, u —the velocity in the liquid phases, r_2 , l_2 —the radius and height of the working zone of the column, t —the time. In the absorption–adsorption cycle, the average outlet concentration of SO₂ in the liquid phase of the absorber is the inlet concentration of SO₂ in the liquid phase of the adsorber [$c_{12}(r_2, 0) \equiv \bar{c}_2(l_1)$], while the average outlet concentration of SO₂ in the liquid phase of the adsorber is the inlet concentration of SO₂ in the liquid phase of the absorber [$c_2(r_1, 0) \equiv \bar{c}_1(l_2)$].

16.2.1 Generalized Analysis

The use of dimensionless (generalized) variables [16, 17] allows to make a qualitative analysis of the models (16.2.1) and (16.2.2), whereas characteristic scales are used the average velocity, the inlet and initial concentrations, the characteristic time t_0 (saturation time of the adsorbent), and the column's dimensions (r_1 , r_2 , l_1 , l_2):

$$\begin{aligned} T &= \frac{t}{t_0}, & R_1 &= \frac{r_1}{r_{10}}, & R_2 &= \frac{r_2}{r_{20}}, & Z &= \frac{z}{l_2}, & Z_1 &= \frac{z_1}{l_1}, & Z_2 &= \frac{z_2}{l_1}, \\ U &= \frac{u}{u^0}, & U_1 &= \frac{u_1}{u_1^0}, & U_2 &= \frac{u_2}{u_2^0}, & C_1 &= \frac{c_1}{c_1^0}, & C_2 &= \frac{c_2 \chi}{c_1^0}, \\ C_{12} &= \frac{c_{12} \chi}{c_1^0}, & C_{13} &= \frac{c_{13} \chi}{c_1^0}, & C_{23} &= \frac{c_{23}}{c_{23}^0}. \end{aligned} \quad (16.2.3)$$

When (16.2.3) is put into (16.2.1) and (16.2.2), the models in generalized variables take the form:

$$\begin{aligned} \gamma_1 \frac{\partial C_1}{\partial T} + U_1 \frac{\partial C_1}{\partial Z_1} &= F_{o1} \left(\beta_1 \frac{\partial^2 C_1}{\partial Z_1^2} + \frac{1}{R_1} \frac{\partial C_1}{\partial R_1} + \frac{\partial^2 C_1}{\partial R_1^2} \right) - K_1(C_1 - C_2); \\ \gamma_2 \frac{\partial C_2}{\partial T} + U_2 \frac{\partial C_2}{\partial Z_2} &= F_{o2} \left(\beta_1 \frac{\partial^2 C_2}{\partial Z_2^2} + \frac{1}{R_1} \frac{\partial C_2}{\partial R_1} + \frac{\partial^2 C_2}{\partial R_1^2} \right) + K_2(C_1 - C_2); \\ T = 0, & \quad C_1 \equiv 1, \quad C_2 \equiv 0; \\ R_1 = 0, & \quad \frac{\partial C_1}{\partial R_1} = \frac{\partial C_2}{\partial R_1} \equiv 0; \quad R_1 = 1, \quad \frac{\partial C_1}{\partial R_1} = \frac{\partial C_2}{\partial R_1} \equiv 0; \\ Z_1 = 0, & \quad C_1(R_1, 0) \equiv 1, \quad 1 \equiv U_1(R_1) - Pe_1^{-1} \left(\frac{\partial C_1}{\partial Z_1} \right)_{Z_1=0}; \\ Z_2 = 0, & \quad C_2(R_1, 0) \equiv \bar{C}_{12}(1), \quad 1 \equiv U_2(R_1) - \frac{Pe_2^{-1}}{\bar{C}_{12}(1)} D_2 \left(\frac{\partial C_2}{\partial Z_2} \right)_{Z_2=0}. \end{aligned} \quad (16.2.4)$$

$$\begin{aligned}
\gamma_0 \frac{\partial C_{12}}{\partial T} + U \frac{\partial C_{12}}{\partial Z} &= F_{00} \left(\beta_0 \frac{\partial^2 C_{12}}{\partial Z^2} + \frac{1}{R_2} \frac{\partial C_{12}}{\partial R_2} + \frac{\partial^2 C_{12}}{\partial R_2^2} \right) - K_0 (C_{12} - C_{13}); \\
\frac{dC_{13}}{dT} &= K_3 (C_{12} - C_{13}) - K_4 C_{13} C_{23} = 0; \quad \frac{dC_{23}}{dT} = -K_5 C_{13} C_{23}; \\
T &= 0, \quad C_{12} \equiv 0, \quad C_{13} \equiv 0, \quad C_{23} \equiv 1; \\
R_2 &= 0, \quad \frac{\partial C_{12}}{\partial R_2} \equiv 0; \quad R_2 = 1, \quad \frac{\partial C_{12}}{\partial R_2} \equiv 0; \\
Z &= 0, \quad C_{12}(R_2, 0) \equiv \bar{C}_2(1), \quad 1 \equiv U(R_2) - \frac{Pe_0^{-1}}{\bar{C}_2(1)} \left(\frac{\partial C_{12}}{\partial Z} \right)_{Z=0}.
\end{aligned} \tag{16.2.5}$$

The following parameters are used in (16.2.4) and (16.2.5):

$$\begin{aligned}
K_0 &= \frac{k_1 l_2}{u^0}, \quad K_1 = \frac{k_0 l_1}{u_1^0}, \quad K_2 = \frac{k_0 l_1 \chi}{u_2^0}, \\
K_3 &= k_1 t_0, \quad K_4 = k t_0 c_{23}^0, \quad K_5 = k t_0 \frac{c_1^0}{\chi}, \\
\gamma_0 &= \frac{l_2}{t_0 u^0}, \quad \gamma_1 = \frac{l_1}{t_0 u_1^0}, \quad \gamma_2 = \frac{l_1}{t_0 u_2^0}, \quad \beta_0 = \frac{r_{20}^2}{l_2^2}, \quad \beta_1 = \frac{r_{10}^2}{l_1^2}, \\
F_{00} &= \frac{D_2 l_2}{u^0 r_{20}^2}, \quad F_{01} = \frac{D_1 l_1}{u_1^0 r_{10}^2}, \quad F_{02} = \frac{D_2 l_1}{u_2^0 r_{10}^2}, \\
\bar{C}_2(1) &= 2 \int_0^1 R_1 C_2(R_1, 1) dR_1, \quad \bar{C}_{12}(1) = 2 \int_0^1 R_2 C_{12}(R_2, 1) dR_2.
\end{aligned} \tag{16.2.6}$$

For lengthy processes ($0 = \gamma_0 \sim \gamma_1 \sim \gamma_2 \leq 10^{-2}$), high columns ($0 = \beta_0 \sim \beta_1 \leq 10^{-2}$), and typical fluid velocities ($0 = F_{00} \sim F_{01} \sim F_{02} \leq 10^{-2}$), the model has the form:

$$\begin{aligned}
U_1 \frac{dC_1}{dZ_1} &= -K_1 (C_1 - C_2); \quad Z_1 = 0, \quad C_1(R_1, 0) \equiv 1. \\
U_2 \frac{dC_2}{dZ_2} &= K_2 (C_1 - C_2); \quad Z_2 = 0, \quad C_2(R_1, 0) \equiv \bar{C}_{12}(1).
\end{aligned} \tag{16.2.7}$$

$$\begin{aligned}
U \frac{dC_{12}}{dZ} &= -K_0 (C_{12} - C_{13}); \quad Z = 0, \quad C_{12}(R_2, 0) \equiv \bar{C}_2(1). \\
\frac{dC_{13}}{dT} &= K_3 (C_{12} - C_{13}) - K_4 C_{13} C_{23} = 0; \quad \frac{dC_{23}}{dT} = -K_5 C_{13} C_{23}; \\
T &= 0, \quad C_{13} \equiv 0, \quad C_{23} \equiv 1.
\end{aligned} \tag{16.2.8}$$

16.3 Average-Concentration Model

The presented models (16.2.7) and (16.2.8) show that in the practical cases convective type of models has to be used:

$$\begin{aligned} u_1 \frac{dc_1}{dz_1} &= -k_0(c_1 - \chi c_2); \quad z_1 = 0, \quad c_1(t, r_1, 0) \equiv c_1^0; \\ u_2 \frac{dc_2}{dz_2} &= k_0(c_1 - \chi c_2); \quad z_2 = 0, \quad c_2(t, r_1, 0) \equiv \bar{c}_{12}(t, l_2). \end{aligned} \quad (16.3.1)$$

$$\begin{aligned} u \frac{dc_{12}}{dz} &= -k_1(c_{12} - c_{13}); \quad z = 0, \quad c_{12}(t, r_2, 0) \equiv \bar{c}_2(t, l_1); \\ \frac{dc_{13}}{dt} &= k_1(c_{12} - c_{13}) - k c_{13}c_{23} = 0; \quad \frac{dc_{23}}{dt} = -k c_{13}c_{23}; \\ t = 0, \quad c_{13}(0, r_2, z) &\equiv 0, \quad c_{23}(0, r_2, z) \equiv c_{23}^0. \end{aligned} \quad (16.3.2)$$

The average values of the velocities and concentrations in the column's cross-sectional area can be obtained [16, 17] using the expressions:

$$\begin{aligned} \bar{u} &= \frac{2}{r_{20}^2} \int_0^{r_{20}} r_2 u(r_2) dr_2 = u^0, \quad \bar{u}_1 = \frac{2}{r_{10}^2} \int_0^{r_{10}} r_1 u_1(r_1) dr_1 = u_1^0, \\ \bar{u}_2 &= \frac{2}{r_{10}^2} \int_0^{r_{10}} r_1 u_2(r_1) dr_1 = u_2^0, \quad \bar{c}_1(t, z_1) = \frac{2}{r_{10}^2} \int_0^{r_{10}} r_1 c_1(t, r_1, z_1) dr_1, \\ \bar{c}_2(t, z_2) &= \frac{2}{r_{10}^2} \int_0^{r_{10}} r_1 c_2(t, r_1, z_2) dr_1, \quad \bar{c}_{12}(t, z) = \frac{2}{r_{20}^2} \int_0^{r_{20}} r_2 c_{12}(t, r_2, z) dr_2, \\ c_{13}(t, z) &= \frac{2}{r_{20}^2} \int_0^{r_{20}} r_2 c_{13}(t, r_2, z) dr_2, \quad \bar{c}_{23}(t, z) = \frac{2}{r_{20}^2} \int_0^{r_{20}} r_2 c_{23}(t, r_2, z) dr_2. \end{aligned} \quad (16.3.3)$$

The velocity and concentration distributions in (16.3.1) and (16.3.2) can be presented with the help of the average functions (16.3.3):

$$\begin{aligned} u(r_2) &= \bar{u} \tilde{u}(r_2), \quad u_1(r_1) = \bar{u}_1 \tilde{u}_1(r_1), \quad u_2(r_1) = \bar{u}_2 \tilde{u}_2(r_1), \\ c_1(t, r_1, z_1) &= \bar{c}_1(t, z_1) \tilde{c}_1(t, r_1, z_1), \quad c_2(t, r_1, z_2) = \bar{c}_2(t, z_2) \tilde{c}_1(t, r_1, z_2), \\ c_{12}(t, r_2, z) &= \bar{c}_{12}(t, z) \tilde{c}_{12}(t, r_2, z), \quad c_{13}(t, r_2, z) = \bar{c}_{13}(t, z) \tilde{c}_{13}(t, r_2, z), \\ c_{23}(t, r_2, z) &= \bar{c}_{23}(t, z) \tilde{c}_{23}(t, r_2, z). \end{aligned} \quad (16.3.4)$$

Here $\tilde{u}(r_2)$, $\tilde{u}_1(r_1)$, $\tilde{u}_2(r_1)$, $\tilde{c}_1(t, r_1, z_1)$, $\tilde{c}_2(t, r_1, z_2)$, $\tilde{c}_{12}(t, r_2, z)$, $\tilde{c}_{13}(t, r_2, z)$, $\tilde{c}_{23}(t, r_2, z)$ present the radial non-uniformity of the velocity and the concentration distributions, satisfying the conditions:

$$\begin{aligned} \frac{2}{r_{20}^2} \int_0^{r_{20}} r_2 \tilde{u}(r_2) dr_2 &= 1, & \frac{2}{r_{10}^2} \int_0^{r_{10}} r_1 \tilde{u}_1(r_1) dr_1 &= 1, & \frac{2}{r_{10}^2} \int_0^{r_{10}} r_1 \tilde{u}_2(r_1) dr_1 &= 1, \\ \int_0^{r_{10}} r_1 \tilde{c}_1(t, r_1, z_1) dr_1 &= 1, & \frac{2}{r_{10}^2} \int_0^{r_{10}} r_1 \tilde{c}_2(t, r_1, z_2) dr_1 &= 1, \\ \frac{2}{r_{20}^2} \int_0^{r_{20}} r_2 \tilde{c}_{12}(t, r_2, z) dr_2 &= 1, & \frac{2}{r_{20}^2} \int_0^{r_{20}} r_2 \tilde{c}_{13}(t, r_2, z) dr_2 &= 1, \\ \frac{2}{r_{20}^2} \int_0^{r_{20}} r_2 \tilde{c}_{23}(t, r_2, z) dr_2 &= 1. \end{aligned} \tag{16.3.5}$$

The use of averaging procedure (II.6–II.10) leads to:

$$\begin{aligned} \alpha_1 \bar{u}_1 \frac{d\bar{c}_1}{dz_1} + \frac{d\alpha_1}{dz_1} \bar{u}_1 \bar{c}_1 &= -k_0(\bar{c}_1 - \chi \bar{c}_2); & z_1 = 0, & \bar{c}_1(t, 0) \equiv c_1^0; \\ \alpha_2 \bar{u}_2 \frac{d\bar{c}_2}{dz_2} + \frac{d\alpha_2}{dz_2} \bar{u}_2 \bar{c}_2 &= k_0(\bar{c}_1 - \chi \bar{c}_2); & z_2 = 0, & \bar{c}_2(t, 0) \equiv \bar{c}_{12}(t, l_2). \end{aligned} \tag{16.3.6}$$

$$\begin{aligned} \alpha \bar{u} \frac{d\bar{c}_{12}}{dz} + \frac{d\alpha}{dz} \bar{u} \bar{c}_{12} &= -k_1(\bar{c}_{12} - \bar{c}_{13}); & z = 0, & \bar{c}_{12}(t, 0) \equiv \bar{c}_2(t, l_1); \\ \frac{d\bar{c}_{13}}{dt} &= k_1(\bar{c}_{12} - \bar{c}_{13}) - \beta k \bar{c}_{13} \bar{c}_{23} = 0; & \frac{d\bar{c}_{23}}{dt} &= -\beta k \bar{c}_{13} \bar{c}_{23}; \\ t = 0, & \bar{c}_{13}(0, z) \equiv 0, & \bar{c}_{23}(0, z) &\equiv c_{23}^0. \end{aligned} \tag{16.3.7}$$

The following functions are used in (16.3.6) and (16.3.7):

$$\begin{aligned} \alpha(t, z) &= \frac{2}{r_{20}^2} \int_0^{r_{20}} r_2 \tilde{u}(r_2) \tilde{c}_{12}(t, r_2, z) dr_2, \\ \alpha_1(t, z_1) &= \frac{2}{r_{10}^2} \int_0^{r_{10}} r_1 \tilde{u}_1(r_1) \tilde{c}_1(t, r_1, z_1) dr_1, \end{aligned}$$

$$\begin{aligned}\alpha_2(t, z_2) &= \frac{2}{r_{10}^2} \int_0^{r_{10}} r_1 \tilde{u}_2(r_1) \tilde{c}_2(t, r_1, z_2) dr_1, \\ \beta(t, z) &= \frac{2}{r_{20}^2} \int_0^{r_{20}} r_2 \tilde{c}_{13}(t, r_2, z) \tilde{c}_{23}(t, r_2, z) dr_2.\end{aligned}\tag{16.3.8}$$

16.3.1 Generalized Analysis

The use of the dimensionless (generalized) variables

$$\begin{aligned}T &= \frac{t}{t_0}, \quad Z = \frac{z}{l_2}, \quad Z_1 = \frac{z_1}{l_1}, \quad Z_2 = \frac{z_2}{l_1}, \\ \bar{C}_1 &= \frac{\bar{c}_1}{c_1^0}, \quad \bar{C}_2 = \frac{\bar{c}_2 \chi}{c_1^0}, \quad \bar{C}_{12} = \frac{\bar{c}_{12} \chi}{c_1^0}, \quad \bar{C}_{13} = \frac{\bar{c}_{13} \chi}{c_1^0}, \quad \bar{C}_{23} = \frac{\bar{c}_{23}}{c_{23}^0}.\end{aligned}\tag{16.3.9}$$

leads to

$$\begin{aligned}A_1 \frac{d\bar{C}_1}{dZ_1} + \frac{dA_1}{dZ_1} \bar{C}_1 &= -K_1(\bar{C}_1 - \bar{C}_2); \quad Z_1 = 0, \quad \bar{C}_1(T, 0) \equiv 1; \\ A_2 \frac{d\bar{C}_2}{dZ_2} + \frac{dA_2}{dZ_2} \bar{C}_2 &= K_2(\bar{C}_1 - \bar{C}_2); \quad Z_2 = 0, \quad \bar{C}_2(T, 0) \equiv \bar{C}_{12}(T, 1).\end{aligned}\tag{16.3.10}$$

$$\begin{aligned}A \frac{d\bar{C}_{12}}{dZ} + \frac{dA}{dZ} \bar{C}_{12} &= -K_0(\bar{C}_{12} - \bar{C}_{13}); \quad Z = 0, \quad \bar{C}_{12}(T, 0) \equiv \bar{C}_2(T, 1); \\ \frac{d\bar{C}_{13}}{dT} &= K_3(\bar{C}_{12} - \bar{C}_{13}) - BK_4 \bar{C}_{13} \bar{C}_{23} = 0; \quad \frac{d\bar{C}_{23}}{dT} = -BK_5 \bar{C}_{13} \bar{C}_{23}; \\ T = 0, \quad \bar{C}_{13}(0, Z) &\equiv 0, \quad \bar{C}_{23}(0, Z) \equiv 1.\end{aligned}\tag{16.3.11}$$

The following functions are used in (16.3.10) and (16.3.11):

$$\begin{aligned}A(T, Z) &= \alpha(t_0 T, l_2 Z) = \alpha(t, z) = 2 \int_0^1 RU(R_2) \frac{C_{12}(T, R_2, Z)}{\bar{C}_{12}(T, Z)} dR_2 \\ A_1(T, Z_1) &= \alpha_1(t_0 T, l_1 Z_1) = \alpha_1(t, z_1) = 2 \int_0^1 R_1 U_1(R_1) \frac{C_1(T, R_1, Z_1)}{\bar{C}_1(T, Z_1)} dR_1\end{aligned}$$

$$\begin{aligned}
A_2(T, Z_2) &= \alpha_2(t_0 T, l_1 Z_2) = \alpha_2(t, z_2) = 2 \int_0^1 R_1 U_2(R_1) \frac{C_2(T, R_1, Z_2)}{\bar{C}_2(T, Z_2)} dR_1 \\
B(T, Z) &= \beta(t_0 T, l_2 Z) = \beta(t, z) = 2 \int_0^1 R_2 \frac{C_{13}(T, R_2, Z)}{\bar{C}_{13}(T, Z)} \frac{C_{23}(T, R_2, Z)}{\bar{C}_{23}(T, Z)} dR_2, \\
\bar{C}_1(T, Z_1) &= 2 \int_0^1 R_1 C_1(T, R_1, Z_1) dR_1, \quad \bar{C}_2(T, Z_2) = 2 \int_0^1 R_1 C_2(T, R_1, Z_2) dR_1, \\
\bar{C}_{13}(T, Z) &= 2 \int_0^1 R_2 C_{13}(T, R_2, Z) dR_2, \quad \bar{C}_{23}(T, Z) = 2 \int_0^1 R_2 C_{23}(T, R_2, Z) dR_2.
\end{aligned} \tag{16.3.12}$$

In Chap. 5, it was shown that $B(T, Z) \equiv 1$ and $A(T, Z)$, $A_1(T, Z_1)$, $A_2(T, Z_2)$ can be presented as linear approximations:

$$A = 1 + a_z Z + a_t T, \quad A_1 = 1 + a_z^1 Z_1 + a_t^1 T, \quad A_2 = 1 + a_z^2 Z_2 + a_t^2 T. \tag{16.3.13}$$

As a result, the model of the absorption-desorption process has the form:

$$\begin{aligned}
(1 + a_z^1 Z_1 + a_t^1 T) \frac{d\bar{C}_1}{dZ_1} + a_z^1 \bar{C}_1 &= -K_1 (\bar{C}_1 - \bar{C}_2); \\
Z_1 = 0, \quad \bar{C}_1(T, 0) &\equiv 1;
\end{aligned} \tag{16.3.14}$$

$$\begin{aligned}
(1 + a_z^2 Z_2 + a_t^2 T) \frac{d\bar{C}_2}{dZ_2} + a_z^2 \bar{C}_2 &= K_2 (\bar{C}_1 - \bar{C}_2); \\
Z_2 = 0, \quad \bar{C}_2(T, 0) &\equiv \bar{C}_{12}(T, 1).
\end{aligned}$$

$$\begin{aligned}
(1 + a_z Z + a_t T) \frac{d\bar{C}_{12}}{dZ} + a_z \bar{C}_{12} &= -K_0 (\bar{C}_{12} - \bar{C}_{13}); \\
Z = 0, \quad \bar{C}_{12}(T, 0) &\equiv \bar{C}_2(T, 1); \\
\frac{d\bar{C}_{13}}{dT} &= K_3 (\bar{C}_{12} - \bar{C}_{13}) - K_4 \bar{C}_{13} \bar{C}_{23} = 0; \\
\frac{d\bar{C}_{23}}{dT} &= -K_5 \bar{C}_{13} \bar{C}_{23}; \\
T = 0, \quad \bar{C}_{13}(0, Z) &\equiv 0, \quad \bar{C}_{23}(0, Z) \equiv 1.
\end{aligned} \tag{16.3.15}$$

16.3.2 Algorithm of the Solution

The solution of (16.3.14) and (16.3.15) can be obtained as five matrix forms:

$$\begin{aligned} \bar{C}_1(T, Z) &= \|C_{(1)\tau\zeta}\|, & \bar{C}_2(T, Z) &= \|C_{(2)\tau\zeta}\|, & \bar{C}_{12}(T, Z) &= \|C_{(12)\tau\zeta}\|, \\ \bar{C}_{13}(T, Z) &= \|C_{(13)\tau\zeta}\|, & \bar{C}_{23}(T, Z) &= \|C_{(23)\tau\zeta}\|; \\ 0 \leq T \leq 1, & \quad T = \frac{\tau - 1}{\tau^0 - 1}, & \quad \tau &= 1, 2, \dots, \tau^0; \\ 0 \leq Z \leq 1, & \quad Z = \frac{\zeta - 1}{\zeta^0 - 1}, & \quad \zeta &= 1, 2, \dots, \zeta^0; \quad \tau^0 = \zeta^0. \end{aligned} \tag{16.3.16}$$

A multi-step approach is possible to be used. At each step, the problems (16.3.14) and (16.3.15) have to be solved consecutively, where T is a parameter in (16.3.14), Z is a parameter in (16.3.15), $\bar{C}_2^{(s)}(T, 0) \equiv \bar{C}_{12}^{(s-1)}(T, 1)$, $\bar{C}_{12}^{(0)}(T, 1) \equiv 0$, where the superscript values ($s = 0, 1, 2, \dots$) are the step numbers.

16.3.3 Parameter Identification

The availability of experimental data for the SO_2 concentrations in the gas and liquid phases at the absorber and adsorber outlets $\bar{C}_1^{\text{exp}}(T_n, 1)$, $\bar{C}_{12}^{\text{exp}}(T_n, 1)$, $T_n = 0.05n$, $n = 1, 2, \dots, 20$ permits to use the next algorithm for the parameter identification in the model (16.3.14) and (16.3.15):

1. Put $a_z = a_t = a_z^1 = a_t^1 = a_z^2 = a_t^2 = 0$ in (16.3.14) and (16.3.15) and minimize the least squares functions:

$$\begin{aligned} F_1(K_1, K_2) &= \sum_{n=1}^{20} [\bar{C}_1(T_n, 1) - \bar{C}_1^{\text{exp}}(T_n, 1)]^2, \\ F_2(K_0, K_3, K_4, K_5) &= \sum_{n=1}^{20} [\bar{C}_{12}(T_n, 1) - \bar{C}_{12}^{\text{exp}}(T_n, 1)]^2, \end{aligned} \tag{16.3.17}$$

where $\bar{C}_1(T_n, 1)$, $\bar{C}_{12}(T_n, 1)$ are obtained as a solution of (16.3.14) and (16.3.15) for $T_n = 0.05n$, $n = 1, 2, \dots, 20$.

2. Enter the obtained parameter values (K_p , $p = 0, 1, \dots, 5$) in (16.3.14) and (16.3.15) and minimize the least squares functions:

$$F_3(a_z^1, a_t^1, a_z^2, a_t^2) = \sum_{n=1}^{20} [\bar{C}_1(T_n, 1) - \bar{C}_1^{\text{exp}}(T_n, 1)]^2, \quad (16.3.18)$$

$$F_4(a_z, a_t) = \sum_{n=1}^{20} [\bar{C}_{12}(T_n, 1) - \bar{C}_{12}^{\text{exp}}(T_n, 1)]^2,$$

where $\bar{C}_1(T_n, 1)$, $\bar{C}_{12}(T_n, 1)$ are obtained as a solution of (16.3.14) and (16.3.15) for $T_n = 0.05n$, $n = 1, 2, \dots, 20$.

3. Enter the calculated values of the parameters $a_z, a_t, a_z^1, a_t^1, a_z^2, a_t^2$ in (16.3.14) and (16.3.15) and minimize the least squares functions (16.3.17), etc.

The proposed patent [15] makes it possible to create a waste-free technology for waste gas purification from sulfur dioxide by means of regenerable absorbent and adsorbent. The proposed method [18] permits to use the absorption columns, where the CaCO_3 suspensions are used.

16.4 An Absorption–Adsorption Apparatus

In the proposed absorption–adsorption method for waste gas purification from sulfur dioxide, the absorption is realized in the countercurrent absorber (where practical gas velocity does not exceed 5 m s^{-1}) and the adsorption is carried out in a fixed bed adsorbent. The efficiency of the process can be increased if the absorption is realized in co-current flows, and the adsorption takes place in the flexible adsorbent. For this, it can use a new absorption–adsorption apparatus with bubbling plates. The bubbling of the gas at a plate through a layer of aqueous suspension of synthetic anionite allows an increasing of the gas velocity (reduction of the diameter of the absorption column), elimination of the adsorption column, and carrying out the adsorption in a flexible adsorbent. The movement of the gas between the plates leads to mixing in the gas phase, which increases the absorption rate because the absorption of sulfur dioxide in water is limited by mass transfer in the gas phase.

The new absorption–adsorption apparatus with bubble plates [19, 20] is shown in Fig. 16.2. The gas enters tangentially into the column 1 through the inlet 2, passes through the distribution pipes 5, concentric bubble caps 6 of the plates 4, and exits the column through the outlet 3. The aqueous suspension of synthetic anionite enters the column 1 via the valve 11 and the pipes 7 and creates of plates 4 layer with a certain thickness. After saturation of the adsorbent with sulfur dioxide, the aqueous suspension is output from the column through the pipes 8 and valves 11 and enters in the system 9 for the regeneration of the adsorbent. The suspension of the regenerated adsorbent is removed from 9 by pump 10 is returned to the plates 4 in the column 1.

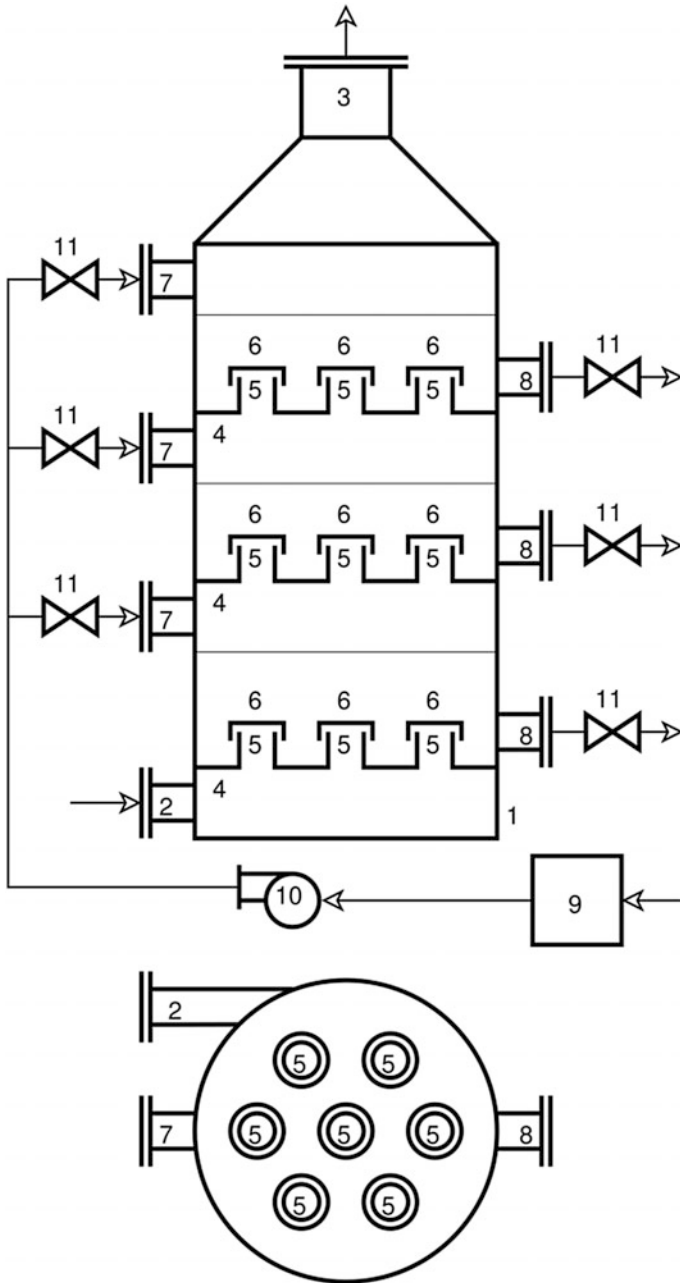


Fig. 16.2 Absorption-adsorption plates column

The operation of the absorption–adsorption apparatus is the following cyclic scheme:

1. Supply all the plates with the necessary amount (volume) of aqueous suspension of synthetic anionite.
2. Start the absorption–adsorption process and monitor the SO_2 concentration of the exit 3.
3. When the increasing the SO_2 concentration at the outlet of the gas 3 exceeds permissible limits, the suspension of the first (bottom) plate is transferred in the regeneration system 9, and the plate is loaded with a new (regenerated) suspension.
4. When the increasing the SO_2 concentration at the outlet of the gas 3 exceeds permissible limits, the suspension of the second (next) plate is transferred in the regeneration system 9, and the plate is loaded with a new (regenerated) suspension.
5. The procedures are repeated until reaching the top plate, then starts again from the first plate.

16.5 Absorption–Adsorption Process Modeling

Tangentially, supplying the gas in the column [19, 21, 22] reduces the radial non-uniformity of the velocity at the column cross-sectional area and the gas velocity is a constant ($u_1 = \text{const.}$), practically. Under these conditions, the concentration of SO_2 in the gas phase is changed only in the height of the column ($c_{11} = c_{11}(t, x)$), which increases the rate of mass transfer rate. On the other hand, the gas bubbling creates an ideal mixing regime in the liquid phase and the concentration of SO_2 in the liquid phase is $c_{12} = c_{12}(t)$. The concentration of SO_2 in the solid phase (capillaries) is c_{13} , and the concentration of active sites in the adsorbent is c_{23} .

The interphase mass transfer rate of SO_2 from the gas to the liquid is $k_0(c_{11} - \chi c_{12})$, while the liquid to the adsorbent is $k_1(c_{12} - c_{13})$. The chemical reaction rate of the SO_2 with the adsorbent is $k c_{13} c_{23}$.

The modeling of a non-stationary (as a result of the adsorbent saturation) absorption–adsorption process on the plate number n ($n = 1, \dots, N$), for gas purification from SO_2 [20], uses a combination of the physical absorption model (3.1.2) and (3.1.3) and chemical adsorption model (3.2.18) and (3.2.19), i.e.,

$$\begin{aligned}
\frac{\partial c_{11}^{(n)}}{\partial t} + u_1 \frac{\partial c_{11}^{(n)}}{\partial z} &= D_1 \frac{\partial^2 c_{11}^{(n)}}{\partial z^2} - k_0 \left(c_{11}^{(n)} - \chi c_{12}^{(n)} \right); \\
\frac{dc_{13}^{(n)}}{dt} &= k_1 \left(c_{12}^{(n)} - c_{13}^{(n)} \right) - k c_{13}^{(n)} c_{23}^{(n)}; \quad \frac{dc_{23}^{(n)}}{dt} = -k c_{13}^{(n)} c_{23}^{(n)}; \\
t = 0, \quad c_{11}^{(n)} &\equiv c_{11}^0, \quad c_{13}^{(n)} \equiv 0, \quad c_{23}^{(n)} \equiv c_{23}^0; \\
z = 0, \quad c_{11}^{(n)}(0) &\equiv c_{11}^{(n-1)}(l), \quad 0 \equiv \left(\frac{\partial c_{11}^{(n)}}{\partial z} \right)_{z=0}, \quad c_{11}^{(1)}(0) \equiv c_{11}^0; \\
n &= 1, \dots, N.
\end{aligned} \tag{16.5.1}$$

In (16.5.1), $z=0$ is the entrance to the gas input of the plate number n ($n=1, \dots, N$), l is the distance between the plates, D_1 is the diffusivity of SO_2 in the gas phase.

The concentration of SO_2 in the water of each plate is determined by the amount of absorbed SO_2 (W_1) and its distribution between liquid phase (W_2), the solid phase (capillaries) (W_3^1) and adsorbed on the surface of the capillaries is (W_3^2):

$$\begin{aligned}
W_1 &= V_1 \left[c_{11}^{(n)}(0) - c_{11}^{(n)}(l) \right], \quad W_2 = V_2 c_{12}^{(n)}, \\
W_3^1 &= V_3 c_{13}^{(n)}, \quad W_3^2 = V_3 \left(c_{23}^0 - c_{23}^{(n)} \right),
\end{aligned} \tag{16.5.2}$$

i.e.,

$$c_{12}^{(n)} = \frac{V_1 \left[c_{11}^{(n)}(0) - c_{11}^{(n)}(l) \right] - V_3 c_{13}^{(n)} - V_3 \left(c_{23}^0 - c_{23}^{(n)} \right)}{V_2}, \tag{16.5.3}$$

16.5.1 Generalized Analysis

The use of dimensionless (generalized) variables [16, 17] allows to make a qualitative analysis of the models (16.5.1) and (16.5.3), whereas characteristic scales are used the inlet and initial concentrations, the characteristic time t_0 (saturation time of the adsorbent) and the distance between the plates l :

$$\begin{aligned}
T &= \frac{t}{t_0}, \quad Z = \frac{z}{l}, \quad C_{11} = \frac{c_{11}}{c_{11}^0}, \\
C_{12} &= \frac{c_{12} \chi}{c_{11}^0}, \quad C_{13} = \frac{c_{13} \chi}{c_{11}^0}, \quad C_{23} = \frac{c_{23}}{c_{23}^0}.
\end{aligned} \tag{16.5.4}$$

When (16.5.4) is put into (16.5.1) and (16.5.3), the model in generalized variables takes the form:

$$\begin{aligned} \gamma \frac{\partial C_{11}^{(n)}}{\partial T} + \frac{\partial C_{11}^{(n)}}{\partial Z} &= Pe^{-1} \frac{d^2 C_{11}^{(n)}}{dZ^2} - K_0 \left(C_{11}^{(n)} - C_{12}^{(n)} \right); \\ \frac{dC_{13}^{(n)}}{dT} &= K_1 \left(C_{12}^{(n)} - C_{13}^{(n)} \right) - KC_{13}^{(n)} C_{23}^{(n)}; \quad \frac{dC_{23}^{(n)}}{dT} = -K\alpha^{-1} C_{13}^{(n)} C_{23}^{(n)}; \\ T = 0, \quad C_{11}^{(n)} &\equiv 1, \quad C_{13}^{(n)} \equiv 0, \quad C_{23}^{(n)} \equiv 1. \end{aligned} \tag{16.5.5}$$

$$Z = 0, \quad C_{11}^{(n)}(0) \equiv C_{11}^{(n-1)}(1), \quad 0 \equiv \left(\frac{dC_{11}^{(n)}}{dZ} \right)_{Z=0}, \quad C_{11}^{(1)}(0) \equiv 1;$$

$n = 1, \dots, N.$

$$C_{12}^{(n)} = \frac{\chi V_1 \left[C_{11}^{(n)}(0) - C_{11}^{(n)}(l) \right] - V_3 C_{13}^{(n)} - \alpha V_3 \left(1 - C_{23}^{(n)} \right)}{V_2}, \quad n = 1, \dots, N. \tag{16.5.6}$$

The following parameters are used in (16.5.5) and (16.5.6):

$$\begin{aligned} Pe &= \frac{u_1 l}{D_1}, \quad K = kt_0 c_{23}^0, \quad K_0 = \frac{k_0 l}{u_1}, \quad K_1 = k_1 t_0, \\ \alpha &= \frac{\chi c_{23}^0}{c_{11}^0}, \quad \gamma = \frac{l}{t_0 u_1}. \end{aligned} \tag{16.5.7}$$

Practically, $0 = \gamma < 10^{-2}$, $0 = Pe^{-1} < 10^{-2}$ and as a result from (16.5.5) follows:

$$\begin{aligned} \frac{dC_{11}^{(n)}}{dZ} &= -K_0 \left(C_{11}^{(n)} - C_{12}^{(n)} \right); \\ Z = 0, \quad C_{11}^{(n)}(0) &\equiv C_{11}^{(n-1)}(1), \quad C_{11}^{(1)}(0) \equiv 1; \quad n = 1, \dots, N. \end{aligned} \tag{16.5.8}$$

$$\begin{aligned} \frac{dC_{13}^{(n)}}{dT} &= K_1 \left(C_{12}^{(n)} - C_{13}^{(n)} \right) - KC_{13}^{(n)} C_{23}^{(n)}; \quad \frac{dC_{23}^{(n)}}{dT} = -K\alpha C_{13}^{(n)} C_{23}^{(n)}; \\ T = 0, \quad C_{13}^{(n)} &\equiv 0, \quad C_{23}^{(n)} \equiv 1. \end{aligned} \tag{16.5.9}$$

The solution of the equations of the model (16.5.6), (16.5.8), and (16.5.9) uses a two-stage algorithm. In the first stage must be solved the equations for $n = 1$. In the second stage must be applied consistently for every plate the algorithm for $n = 1$.

16.5.2 Algorithm of the Solution

1. Put $n = 1$.
2. Put $C_{12}^{(1)} = X_i = 0.1i$, $i = 1, \dots, 10$.
3. The solution of (16.5.8) leads to $C_{11}^{(1i)} = C_{11}^{(1)}(Z, X_i)$, $C_{11}^{(1)}(0, X_i)$, $C_{11}^{(1)}(1, X_i)$, $i = 1, \dots, 10$.
4. The solution of (16.5.9) leads to $C_{13}^{(1i)} = C_{13}^{(1)}(T, X_i)$, $C_{23}^{(1i)} = C_{23}^{(1)}(T, X_i)$, $i = 1, \dots, 10$.
5. The solutions in 3 and 4 must be introduced in (16.5.6) and as a result is obtained $C_{12}^{(1i)} = C_{12}^{(1)}(T, X_i)$, $i = 1, \dots, 10$.
6. Put $T = T_i = 0.1j$, $j = 1, \dots, 10$ in $C_{12}^{(1i)} = C_{12}^{(1)}(T, X_i)$, $i = 1, \dots, 10$ and as a result is obtained $\bar{C}_{12}^{(1i)} = C_{12}^{(1)}(T_j, X_i)$, $i = 1, \dots, 10$, $j = 1, \dots, 10$.
7. A polynomial approximation $P_{12}^{(1j)}(T_j, X)$, $j = 1, \dots, 10$ of $\bar{C}_{12}^{(1i)} = C_{12}^{(1)}(T_j, X_i)$, $i = 1, \dots, 10$, $j = 1, \dots, 10$ with respect to X must be obtained.
8. The solutions of the equations $X = P_{12}^{(1j)}(T_j, X)$, $j = 1, \dots, 10$ with respect to X permits to be obtained X_j , $j = 1, \dots, 10$ and the obtained solutions must be denoted as $X_j = C_{12}^{(1)}(T_j)$, $j = 1, \dots, 10$.
9. A polynomial approximation of $C_{12}^{(1)}(T_j)$, $j = 1, \dots, 10$ with respect to T permit to be obtained $C_{12}^{(1)}(T) = C_{12}^{(1)}(T_j)$, $j = 1, \dots, 10$.
10. The introducing of $C_{12}^{(1)}(T)$ in (16.5.8) and (16.5.9) permits to be obtained its solutions for $n = 1$.
11. The obtained solution of (16.5.8) $C_{11}^{(1)} = C_{11}^{(1)}(T, Z)$ permits to be obtained $C_{11}^{(1)} = C_{11}^{(1)}(T, 1)$ and as a result to be used the algorithm 1–11 for consistent solutions of the equations set (16.5.6) and (16.5.8) for $n = 2, \dots, N$.

16.5.3 Parameter Identification

The parameters in the model (16.5.6), (16.5.8), and (16.5.9), which are subjected to experimental determination are K , K_0 , K_1 . They may be obtained from experimental data of the SO_2 concentration at the gas outlet from the first plate $C_{11 \text{ exp}}^{(1j)} = C_{11}^{(1)}(T_j, 1)$, $T_i = 0.1j$, $j = 1, \dots, 10$, where $T = 1$ is the time for the full saturation of the adsorbent on the first plate. For this purpose must be minimized the function of the least squares with respect to K , K_0 , K_1 :

$$F(K, K_0, K_1) = \sum_{j=1}^{10} \left[C_{11}^{(1)}(T_j, 1) - \bar{C}_{11 \text{ exp}}^{(1j)} \right]^2. \quad (16.5.10)$$

The proposed utility model [19] uses an absorption–adsorption column and makes it possible to create a waste-free technology for waste gas purification from sulfur dioxide by means of regenerable adsorbent, where the system for the regeneration of the adsorbent is similar to the regeneration system in the patent [15]. The efficiency of the processes is increased in an absorption–adsorption apparatus, where the absorption is realized in co-current flows and the adsorption takes place in the flexible adsorbent. For this is proposed a new absorption–adsorption column apparatus with bubbling plates. A mathematical model of the absorption–adsorption process is presented, too.

References

1. Bruce KR (1989) Comparative SO₂ reactivity of CaO derived from CaCO₃ and Ca(OH)₂. *AIChE J* 35(1):37
2. Fahrenkamp H (1985) Entwicklungstendenzen der Rauchgasentschwerfelungstechnik auf Kalksteinbasis. Vortagsveroff Haus TechEssen no. 490:9
3. Jozewicz W, Kirchgessner DA (1989) Activation and reactivity of novel calcium-based sorbents for dry SO₂—control in boilers. *Power Technol* 58:221
4. Boyadjiev C (2011) Mechanism of gas absorption with two-phase absorbents. *Int J Heat Mass Transfer* 54:3004–3008
5. Boyadjiev C (2011) On the SO₂ problem in power engineering. In: *Proceedings, energy forum, Bulgaria*, p 114–125
6. Boyadjiev C (2012) On the SO₂ problem in power engineering. In: *Proceedings, Asia-Pacific power and energy engineering conference (APPEEC 2012), China*, vol 1
7. Boyadjiev C (2012) On the SO₂ problem of solid fuel combustion. In: *Proceedings, VIII All-Russian conference with international participation “solid fuel combustion”, Novosibirsk*
8. Boyadjiev C, Doichinova M, Popova P (2011) On the SO₂ problem in power engineering. 1. Gas absorption. In: *Proceedings, 15th workshop on transport phenomena in two-phase flow, 94–103, Sunny Beach Resort, Bulgaria*, pp 17–22
9. Boyadjiev C, Popova P, Doichinova M (2011) On the SO₂ problem in power engineering. 2. Two-phase absorbents. *Proceedings, 15th workshop on transport phenomena in two-phase flow, Bulgaria*, pp 104–115
10. Boyadjiev C, Doichinova M, Popova P (2012) On the SO₂ problem in power engineering. *Trans Academenergo* 1:44–65
11. Boyadjiev C, Boyadjiev B, Doichinova M, Popova-Krumova P (2013) Method and apparatus for gas absorption. Patent application No 111168
12. Pantofchieva L, Boyadjiev C (1995) Adsorption of sulphur dioxide by synthetic anion exchangers. *Bulg Chem Comm* 28:780
13. Boyadjiev C, Pantofchieva L, Hristov J (2000) Sulphur dioxide adsorption in a fixed bed of a synthetic anionite. *Theor Found Chem Eng* 34(2):141
14. Hristov J, Boyadjiev C, Pantofchieva L (2000) Sulphur dioxide adsorption in a magnetically stabilized bed of a synthetic anionite. *Theor Found Chem Eng* 34(5):489
15. Boyadjiev C, Boyadjiev B, Doichinova M, Popova-Krumova P (2014) Method and apparatus for gas cleaning from sulfur dioxide. Patent application No 111398
16. Boyadjiev C (2010) *Theoretical chemical engineering. modeling and simulation*. Springer, Berlin
17. Doichinova M, Boyadjiev C (2012) On the column apparatuses modeling. *Int J Heat Mass Transfer* 55:6705–6715

18. Boyadjiev C, Boyadjiev B (2017) An absorption-adsorption method for gases purification from SO₂ in power plants. *Recent Innov in Chem Eng* (in press)
19. Boyadjiev C, Boyadjiev B (2015) Absorption-adsorption apparatus for gas cleaning from sulfur dioxide. *Utility model BG 2196:U1*
20. Boyadjiev C, Boyadjiev B (2017) An absorption-adsorption apparatus for gases purification from SO₂ in power plants. *Open Access Libr J* 4(5):e3546
21. Boyadjiev C, Boyadjiev B (2013) Column reactor for chemical processes. *Utility model BG 1776:U1*
22. Boyadjiev C, Doichinova M, Popova-Krumova P, Boyadjiev B (2014) Intensive column apparatus for chemical reactions. *Open Access Libr J* 1(3):1–9